

# A 'crack-like' notch analogue for a safe-life fretting fatigue design methodology

M. CIAVARELLA

CEMEC—Centro di Eccellenza in Meccanica Computazionale, Politecnico di Bari, Viale Japigia, 182, 70126 Bari, Italy

Received in final form 2 June 2003

**ABSTRACT** Various analogies have recently been proposed for comparing the stress fields induced in fretting fatigue contact situations, with those of a crack and a sharp or a rounded notch, resulting in a degree of uncertainty over which model is most appropriate in a given situation. However, a simple recent approach of Atzori–Lazzarin for infinite-life fatigue design in the presence of a geometrical notch suggests a corresponding unified model also for fretting fatigue (called *Crack-Like Notch Analogue* model) considering only two possible behaviours: either 'crack-like' or 'large blunt notch.' In a general fretting fatigue situation, the former condition is treated with a single contact problem corresponding to a *Crack Analogue* model; the latter, with a simple peak stress condition (as in previous *Notch Analogue* models), simply stating that below the fatigue limit, infinite life is predicted for any size of contact. In the typical situation of constant normal load and in phase oscillating tangential and bulk loads, both limiting conditions can be readily stated. Not only is the model asymptotically correct if friction is infinitely high or the contact area is very small, but also remarkably accurate in realistic conditions, as shown by excellent agreement with Hertzian experimental results on Al and Ti alloys. The model is useful for preliminary design or planning of experiments reducing spurious dependences on an otherwise too large number of parameters. In fact, for not too large contact areas ('crack-like' contact) no dependence at all on geometry is predicted, but only on three load factors (bulk stress, tangential load and average pressure) and size of the contact. Only in the 'large blunt notch' region occurring typically only at very large sizes of contact, does the size-effect disappear, but the dependence is on all other factors including geometry.

**Keywords** fretting fatigue; HCF fatigue; safe-life design.

## NOMENCLATURE

$a$  = notch or crack half-width (i.e., contact half-width)  
 $a_0$  = El Haddad intrinsic crack size  
 $K_f$  = fatigue strength reduction factor  
 $K_{ff} = K_f$  in the region of crack-like fretting fatigue notch behaviour  
 $K_{ft} = K_f$  in the region of blunt fretting fatigue notch behaviour  
 $K_t$  = elastic stress concentration factor  
 $\Delta K_{th}$  = threshold value of the stress intensity factor range  
 $Y$  = geometric or fretting fatigue shape factor  
 $\Delta\sigma$  = range of the gross nominal stress  
 $\Delta\sigma_1$  = plain specimen fatigue limit (in terms of stress range)

## INTRODUCTION

Fretting was originally considered as the process of rubbing two surfaces together producing various surface modifications and damage but, without a mechanical fa-

tigue load applied to the contacting bodies, limited to the very superficial layers of the material.<sup>1</sup> Fretting fatigue (FF) was first recognized in specimens fractured in the grips of fatigue machines,<sup>2,3</sup> but has been studied for a long time as a 'separate' area of fatigue, where the mechanical damage over the surface was considered to have a dominant role in decreasing the fatigue

Correspondence: M. Ciavarella. E-mail: mciava@dimeg.poliba.it

performance of the material. Various attempts to introduce empirical parameters such as microslip amplitude and surface energy dissipated by friction<sup>4–8</sup> have emerged from this background, but have, in the best of the author's knowledge, failed to demonstrate any significant effect not predicted by standard fatigue from a stress-raising feature. Actually, it was recognized that only a small decrease of fatigue performance (13–17%) was obtained in previously fretted specimens,<sup>9</sup> suggesting only the combined effect of fretting and fatigue was causing a significant strength reduction. Finally, experiments in inert gas atmosphere showed that, although fretting decreased, the fretting strength was not significantly increased, confirming that the two processes are independent, and the damaging process is only of minor effect.<sup>10</sup>

Probably, microslip parameters have had some success because they were also an indirect means to measure tangential load in most fretting fixtures, such as bridge-type rigs holding pads or feet of nearly flat geometry. Under such conditions, the effects are intrinsically connected and therefore not always distinct and clear; the number of parameters is too high anyway for a convenient empirical theory to emerge. Damage-related empirical parameters seem now in disuse.<sup>11</sup>

The role of the contact stress field in provoking simply *fatigue from a stress concentration* had been recognized as the most significant feature of the problem in remarkable early papers.<sup>12,13</sup> But only recently have a number of attempts been made,<sup>14</sup> sometimes with methodologies of considerable effort to include multiaxial effects,<sup>15,16</sup> or both multiaxial and size effects.<sup>17,18</sup> Despite the sophistication, only partial success was achieved, either accurate predictions were obtained only for a subset of experiments or empirical fitting constants were used. We shall call this class *Notch Analogue* (NA) models where we intend that the calculation of the actual stress field in the contact problem is computed with accuracy for the given geometry, as a function of friction coefficient inducing partial slip.

Another important attempt to model FF was fracture mechanics based, which probably started in the late 1970s.<sup>19,20</sup> They recognized an initial propagation phase (obviously faster than in plain fatigue) mainly due to shear with a small propagation depth inclined with respect to the surface and the principal stress. After this, a knee point formed where cracks turned to propagate perpendicular to the surface. The first phase depended on the decaying contact field and the second mostly on the more uniform bulk stress field, although this distinction is not rigorous as the combined stress field is the driving force of the cracks. Most of these attempts, as well as later ones,<sup>21</sup> included an initial crack of arbitrary size and orientation, which had to be assumed. Collecting most of these findings, a further step forward was made by Giannakopoulos *et al.*,<sup>22</sup> with the so-called *Crack Analogue* (CA) model, for the case

where the contact is complete (singular pressure and frictional shear tractions), introducing an implicit length scale to the problem, directly justifying the size effect. This was a remarkably simple and attractive model as it removed the dependence on the arbitrary initial flaw size. Despite the idea of using fracture mechanics for contact-induced singular stress fields appears entirely reasonable and almost obvious, it had not been attempted before, perhaps because the negative mode I stress intensity factor was considered an obstacle, or because no perfectly sharp geometry or no exact square root singularity is achieved in practical FF conditions.<sup>22</sup> It is also worth remarking that a further motivation for the use of a Crack Analogue (CA) is adhesion which may also induce singularity in the stress field even for a non-sharp geometry.<sup>24</sup> In particular, for the condition defined as strong adhesion, the mode II stress intensity is practically the same as in the case of infinite friction—leading back to the CA model for a general geometry. Whether adhesion is another way of looking at the experimental fact that friction coefficient seems to rise significantly in the micro-slip areas during fretting, is irrelevant as, in either case, we have strong reasons to hope for success from a CA model.

Many features of the CA model will be reconsidered here, but a few improvements will be made first. In particular, bulk stress was neglected in the computation of stress intensity factors for initiation purposes, whereas self-arrest was given as a condition on the bulk stress *only* affecting the calculation of the kinked crack stress intensity factors, and so the contact stress field was neglected in this phase. These assumptions will be removed and the condition of initiation will be computed more precisely.

The CA and NA models remain somewhere distinct and not fully integrated. Also, the case when the contact area is so small that short crack effects become important was not addressed. In the limit when the contact is vanishing small, the only condition to write is that the bulk stress is smaller than fatigue limit, independently from fretting loads. It will appear in the course of the present paper that a unified treatment not only makes more accurate and clear the resulting predictions, but turns out even simpler than both the original CA and the NA models, permitting simple reasoning over the influence of various factors. The key starting point is that, up to a certain limiting size, notches of all shapes behave very similarly to cracks of the same size ('crack-like' notches, a description first suggested by Smith and Miller<sup>25</sup>), irrespective of minor differences of the form of the stress distribution, and it is only above this size that the peak stress criterion is appropriate. Moreover, in fretting the friction coefficient rapidly grows in the microslip regions of the contact areas. If this does not happen, such as when using anti-friction coatings, it is likely that FF is not a problem. Therefore, given that in the limit of infinite friction any contact

geometry would restore the mode II stress intensity factor of the CA model, it is likely that most fretting contact behaves according to the CA model (at least up to a certain size of contact). When the corresponding problem is correctly solved, we could write very simply the general threshold condition.

The Smith and Miller classification of notches has been best exploited recently by Atzori and Lazzarin<sup>26</sup> using the El Haddad law<sup>27</sup> for the correction at small sizes. Accordingly, the knock-down factor in fatigue,  $K_f$ , has been derived in a unified way, together with the  $K_t$  criterion for larger sizes, and extended to include geometrical effects by Atzori *et al.*<sup>28</sup>

$$K_f = \begin{pmatrix} \sqrt{1 + Y^2 \frac{a}{a_0}}, & \text{for } a < a^* \\ K_t, & \text{for } a > a^* \end{pmatrix} \quad \text{or} \quad (1)$$

$$K_f = \text{Min} \left( \sqrt{1 + Y^2 \frac{a}{a_0}}, K_t \right),$$

where  $a^*$  is the transitional size where the 'crack-like notch' behaviour meets the 'large blunt notch' behaviour ( $Y$  here is the geometrical factor correcting with respect to the ideal case of central crack in a infinite plate)

$$a^* = a_0 \left( \frac{K_t}{Y} \right)^2, \quad (2)$$

where the material constant  $a_0$  is defined for a given threshold stress intensity range  $\Delta K_{th}$  and a fatigue limit  $\Delta \sigma_1$  as

$$a_0 = \frac{1}{\pi} \left( \frac{\Delta K_{th}}{\Delta \sigma_1} \right)^2, \quad (3)$$

which has often the, perhaps misleading, interpretation of 'intrinsic crack' in El Haddad *et al.*<sup>27</sup>

Therefore, by identifying the sharp contact geometry and solving for the given loading condition, we can estimate the factor  $K_f$ , defined as the ratio between fatigue limit and bulk stress load. The contact loadings will be taken care of via the geometrical factor  $Y$  of Eq. (1). Finally, for contact sizes larger than  $a^*$ , the peak stress will be computed. Therefore, improved versions of both CA and NA models will be included in the more comprehensive crack-like notch analogue (CLNA) model using the Atzori and Lazzarin criterion.

**A CA MODEL WITH IMPROVEMENTS**

Consider a square-ended foot pressing a fatigue specimen, according to the geometry in Fig. 1. For a constant mode I normal load  $P$ , and a varying mode II load  $Q$ , we have (for a 2D geometry and an  $R = -1$  loading ratio)

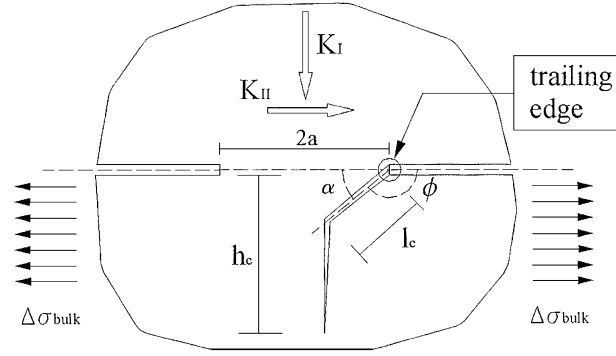


Fig. 1 The CA model a flat punch under normal load.

$$K_I = - \left( \frac{P}{\sqrt{\pi a}} \right) = - \left( \frac{2}{\pi} \bar{p} \sqrt{a} \right), \quad (4)$$

$$\Delta K_{II} = 2 \left( \frac{Q}{\sqrt{\pi a}} \right) = 2 \left( \frac{2}{\pi} \bar{q} \sqrt{a} \right),$$

where  $\Delta$  is the range in the cycle,  $\bar{p} = \frac{P}{2a}$  and  $\bar{q} = \frac{Q}{2a}$ .

Recently, we have improved the analysis of the contact problem in Fig. 1 considered in Ref. [22] by looking directly at the governing integral equations.<sup>29</sup> We assume Dundurs' mismatch constant is zero,  $\beta = 0$ , and that the half-plane elasticity can be used for both materials, which is only rigorous in the case of a rigid punch indenting an incompressible material. The latter condition requires  $E_1 \rightarrow \infty$  and  $\nu_1 \rightarrow 1/2$ , i.e., the constant  $\gamma \rightarrow 1$ , where

$$\gamma = \left( \frac{E_2^*}{E_1^*} + 1 \right) = \left( \frac{1 - \nu_1^2}{E_1} \bigg/ \frac{1 - \nu_2^2}{E_2} \right) + 1. \quad (5)$$

Otherwise, the solution will deviate from the square-root singular one.<sup>23</sup> We shall leave the general case of  $\gamma$  because these deviations would not affect the fatigue strength for an actual contact case except in a restricted range of large contact sizes, yet not enough for the  $K_t$  condition to prevail. In the comparison for Hertzian experiments, for example, we will successfully use the model with identical materials ( $\gamma = 2$ ).

Turning back to the contact problem, in the case of tangential and bulk load applied simultaneously and in phase, three conditions (stick, one slip zone and two slip zones) are found,<sup>29</sup> as indicated in Fig. 2. As we are only interested in the trailing edge stress intensity factors, for which there are only two cases, which should be used instead of the second of Eq. (4) (see Ciavarella and Macina<sup>29</sup>)

$$(K_{II})_{stick} = \left( \frac{Q}{\sqrt{\pi a}} \right) + \frac{1}{2\gamma} \sigma_b \sqrt{\pi a},$$

$$\sigma_b \leq \frac{4}{\pi} \gamma f \bar{p} \left( 1 - \frac{Q}{fP} \right) \quad (6)$$

$$(K_{II})_{stick} = f K_I, \quad \sigma_b > \frac{4}{\pi} \gamma f \bar{p} \left( 1 - \frac{Q}{fP} \right).$$

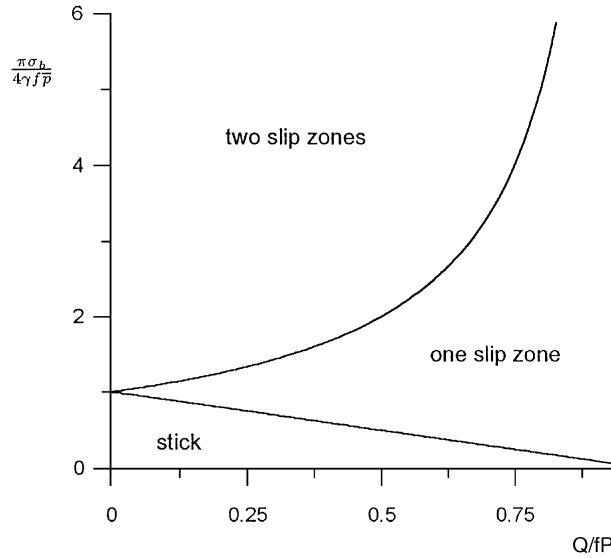


Fig. 2 Partial slip condition in the CA model contact problem, according to the load conditions  $Q/fP$ , and  $(\pi\sigma_b)/(4\gamma f\bar{p})$ .

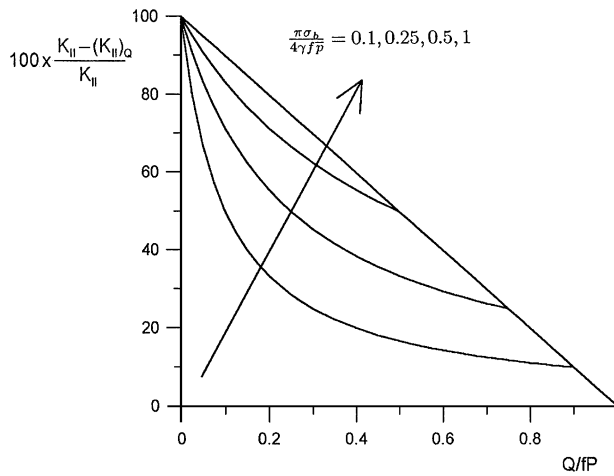


Fig. 3 Correction (in percentage) in the mode II SIF with respect to the original CA model, for  $(\pi\sigma_b)/(4\gamma f\bar{p}) = 0.1, 0.25, 0.5, 1$ .

The new factors are compared with the original CA model,<sup>22</sup> where only the contribution due to the tangential load was taken into account  $K_{II}^Q = Q/\sqrt{(\pi a)}$ . The difference is reported in Fig. 3. Clearly, the error is larger for large bulk loads and low  $Q/fP$ , i.e., away from the friction limit, when the effect of bulk load dominates over the tangential load.

**THE NA MODEL**

For the ‘large blunt notch’ equivalence, we simply need a good estimate of the peak stress. A number of exact results are known from detailed analyses.<sup>30,31</sup> A simple yet

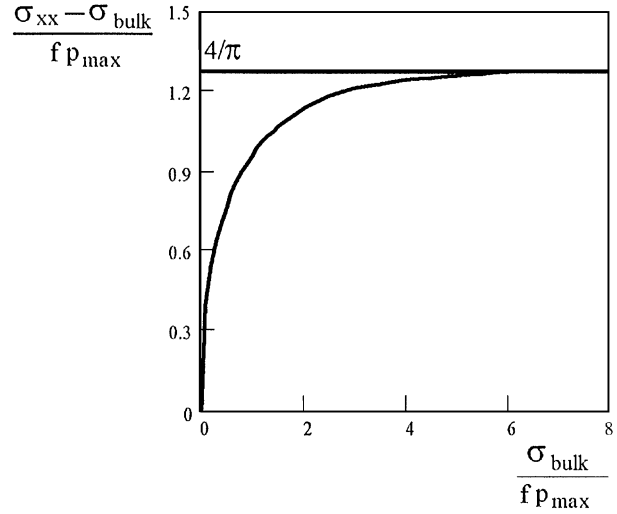


Fig. 4 Hertzian contact with bulk stress only: Difference between  $\sigma_{xx}(a, 0)$  and  $\sigma_b$  as a function of  $\sigma_b$ .

accurate formula for Hertzian, or rounded flat geometry, subject to constant pressure and oscillating tangential load is given by Ciavarella *et al.*<sup>32,33</sup> neglecting the effect of bulk stress on shear tractions,

$$\sigma_{cont} = \frac{8}{\pi} \bar{p} k \sqrt{fQ/P}, \tag{7}$$

where  $k$  is a contact geometrical factor equal to 1 in the Hertz contact case, and increasingly greater for rounded flat geometries towards the flat indenter case ( $d$  is the half-width of the flat part of the punch and  $a$  the half-width of contact)

$$k = \sqrt{\frac{1 - \frac{2}{\pi} \arcsin(\frac{d}{a})}{1 - \frac{2}{\pi} \arcsin(\frac{d}{a}) - \frac{2}{\pi} (\frac{d}{a}) \sqrt{1 - (\frac{d}{a})^2}}}. \tag{8}$$

The above formula is only valid when no bulk stress is considered, and a simple linear superposition is the simplest correction as done, for example, by Giannakopoulos *et al.*,<sup>14</sup> and using (7)

$$\sigma_{max} = \sigma_b + \sigma_{cont} = \sigma_b + \frac{8}{\pi} \bar{p} k \sqrt{fQ/P}. \tag{9}$$

The exact solution for an arbitrary combination of bulk stress and tangential load requires either more sophisticated analytical solutions or numerical methods.<sup>32,33</sup> Figure 4 shows an example of the stress concentration induced under bulk stress only loading conditions for Hertzian contact.

**THE NEW CLNA MODEL**

The original CA model<sup>22</sup> was a remarkably innovative and simple model for FF finding a clear explanation of

the size effect found experimentally. However, it may be questioned that in most contact problems, the corners of the indenters are not perfectly sharp, or even if they are, the singularity is not square root. Indeed, it had been noticed that in many practical fretting conditions, a realistic geometry (e.g., in dovetail or fir-tree attachments of aeronautical turbine engines) could be obtained by rounding the corners of the indenter instead of having a sharp end,<sup>34</sup> showing also that a detailed analytical solution for the contact problem was still possible. In a subsequent paper,<sup>14</sup> it was suggested that the stress field for this finite stress concentration is a perturbation of the limiting case of sharp punch in the CA model, like the Creager-Paris solution for a rounded crack is a perturbation of the crack solution. This notch-analogue (NA) model, however, was not pursued further than suggesting simply the peak stress as a criterion for initiation, although it is well known that in fatigue in the presence of a geometrical notch, the use of the stress concentration factor is a largely conservative condition, valid only asymptotically at large sizes of notches.

In fretting, there are various independent loading conditions, and if only one is changed while the others are kept constant, the peak-stress condition may never be reached, irrespective of how large the contact area is. For example, if the contact stress is kept constant and higher than fatigue limit, the only possible regime is crack-like notch. Similarly, if the bulk stress, or more generally if the sum of the two, is maintained constant and higher than fatigue limit. This will be discussed later in more detail. Classical theories on peak stress and gradient of stress field (like Peterson, Neuber, etc.) do not lead to significantly better prediction than a simple criterion assuming either 'crack-like' or 'large blunt notch' behaviour as recently suggested by Atzori and Lazzarin.<sup>26</sup> The opposite is true since the original Peterson's and Neuber's constants are only based on ultimate strength and do not take into account the fatigue threshold. The most significant contribution to the classical knock-down factor in fatigue,  $K_f$ , is due to the crack-like behaviour, so that a detailed analysis of the stress field around each single case of notch, clearly depending upon the specific geometry, is avoided. The simplicity of the Atzori-Lazzarin criterion turns out particularly helpful in fretting, where there are a number of parameters at play for which other criteria would not permit simple handling of the results.

A generic FF problem is a much more complex situation than the standard geometric notch or crack subject to a remote uniaxial tensile fatigue loading. For the 'remote stress' condition in principle we could consider the bulk stress  $\sigma_b$ , or the pressure  $p$ , or the shear traction  $q \leq fp$ , and similarly in general there may be various mode singularities (possibly all modes I, II, III), under non-proportional conditions. Non-proportionality may depend on the paths

followed by normal tangential and bulk loads, and/or from the contact area variations associated with change of normal load. These factors cannot necessarily be all considered with present models and some degree of simplification is needed. However, by limiting the attention to cases where the normal load is constant and the tangential load is oscillating (the Cattaneo-Mindlin conditions), we realize that the most significant contribution to fatigue life corresponds to oscillating tensile stresses induced by tangential and bulk loads. Therefore, we suggest to take into account only two limiting conditions, combining CA and NA model, in what we define a CLNA model. In particular, for small to intermediate size of contact areas, the bulk stress is the nominal stress, and the stress intensity factor giving rise to fatigue is mode II due to both shear and bulk stress. Notice that the reasons why non-sharp fretting configurations (up to a certain limiting size) can use a crack-like model are somehow *stronger* than in the corresponding notch problem considered in the original Atzori and Lazzarin<sup>26</sup> criterion (which has been nevertheless experimentally validated for most notch geometries in Atzori *et al.*<sup>28</sup>), as there are two additional considerations:

- (1) if friction is very high, an actual mode II stress intensity is introduced by friction, independent of the actual contact geometry;
- (2) if adhesion is high, a singularity in mode I (positive) is induced by adhesion and friction, in principle also if finite, gives rise to an actual mode II singularity, as considered in the paper by Giannakopoulos *et al.*<sup>24</sup>

For larger contact areas, we shall skip to a NA model, as a truncation to the CA-model prediction. It should be noted however that, while for a true notch this condition always occurs at sufficiently large sizes, in FF the peak stress condition is not necessarily reached irrespective of how arbitrarily the contact area is increased. In fact in the FF case, if we consider bulk stress as the nominal stress, there will be a  $K_t$  truncation only if all other conditions are such that bulk plus contact stress equals the fatigue limit. For example we may suppose to increase the contact area, while decreasing the peak pressure proportionally to bulk stress, with the loading ratio  $Q/fP$  kept constant. In this case, also the peak stress will decrease proportionally to bulk nominal stress, as it happens in a geometrical notch. Hence, the truncation will eventually occur as the peak stress at one point will have to be lower than fatigue limit. However, if we consider the case of decreasing the bulk stress in the diagram while peak pressure is maintained constant, then the crack-like condition may always be more severe, and indeed also impose a limit of the contact area dimension which cannot be exceeded for that given peak (or average) pressure. We shall return to this problem later.

**Implementation of the CLNA model: crack-like notch behaviour**

Let us start from the condition of small to intermediate size of contact area. The mode II stress intensity factor depends, according to Eq. (6), on tangential load and bulk stress only (for sticking conditions), or on average pressure and friction coefficient (for sliding conditions). In order to use the El Haddad equation for the transition small crack/small notch, we need to combine the effect of the bulk stress. In the case of moderate bulk, the first part of Eq. (6) needs to be used, i.e., for  $\sigma_b \leq (4/\pi)\gamma f \bar{p}(1 - Q/fP)$ , suggesting that at the maximum load (here we consider only the case of bulk stress and tangential load applied simultaneously and in phase, while keeping normal load constant)

$$K_{II} = (K_{II})_{stick} = \left( \frac{2}{\pi} \bar{q} + \frac{1}{2\gamma} \sigma_b \right) \sqrt{\pi a} = Y \sigma_b \sqrt{\pi a}, \quad (10)$$

where  $Y$  is here a *fictitious geometrical factor* as it is normally used to include geometrical effects with respect to the classical central crack in the infinite plate solution,  $K = \sigma \sqrt{(\pi a)}$ . In this manner, the mode II SIF has been written in terms of the bulk stress instead of the mean shear traction. The factor  $Y$ , differently from a true geometrical factor in standard fracture mechanics, is here a factor depending on loading condition. Specifically, from the equation above,

$$Y_{stick} \left( \sigma_b, \bar{p}, \frac{Q}{P} \right) = \frac{2}{\pi} \frac{\bar{p}}{\sigma_b} Q/P + \frac{1}{2\gamma}, \quad (11)$$

whereas for larger bulk, the second part of Eq. (6) should be used, and so

$$Y_{slip}(\sigma_b, \bar{p}, f) = \frac{2}{\pi} \frac{f \bar{p}}{\sigma_b}. \quad (12)$$

We are now in a position to write down the El Haddad equation in the form suggested by Atzori–Lazzarin<sup>26</sup> and Atzori *et al.*<sup>28</sup> taking into account the geometrical factor asymptotics and by defining  $K_{ff}$  as the ratio

$$K_{ff} = \frac{\Delta \sigma}{\Delta \sigma_b} = \sqrt{1 + Y^2 \frac{a}{a_0}}. \quad (13)$$

This expression clearly considers the two threshold conditions: fatigue limit for the nominal bulk stress  $\sigma_b$ , in the limit as  $a = 0$ , and long-crack fatigue threshold condition, when  $a \rightarrow \infty$ . In contrast to standard fatigue cases then, this equation contains a factor  $Y$ , which depends on loads and on the fatigue stress itself, specifically on  $\sigma_b$ . Therefore, this dependency means that the equation above is in fact an implicit equation for  $K_{ff}$ , in general. However, supposing the two ratios

$$R_p = \frac{\bar{p}}{\sigma_b}, \quad R_q = \frac{Q}{P} \quad (14)$$

and  $f$  are maintained constants, we rewrite Eqs (11) and (12) as

$$Y_{stick}(R_p, R_q) = \frac{2}{\pi} R_p R_q + \frac{1}{2\gamma}; \quad (15)$$

$$Y_{slip}(R_p, f) = \frac{2}{\pi} R_p f.$$

In practise, the two  $Y$ 's can be both computed, but only the smallest used in the calculations. Rewriting Eq. (13) with emphasis on explicit dependences on the various factors,

$$K_{ff} \left( R_p, R_q; f, \frac{a}{a_0} \right) = \sqrt{1 + \left\langle \frac{2}{\pi} R_p R_q + \frac{1}{2\gamma}; \frac{2}{\pi} R_p f \right\rangle^2 \frac{a}{a_0}}, \quad (16)$$

where  $\langle a; b \rangle$  indicates the minimum between  $a, b$ . Notice that  $K_{ff}$  in the final form of Eq. (16) depends on three non-dimensional factors only: the pressure ratio  $R_p$  and either the tractive ratio  $R_q$  or the friction coefficient  $f$ , and the crack ratio,  $a/a_0$ .

**Implementation of the CLNA model: blunt notch behaviour**

Turning back to the peak stress condition, a simple estimate of the tensile stress at the trailing edge of contact can be given for Hertzian or rounded flat contact without considering the nonlinear effect of bulk stress affecting the traction distribution, as (Ciavarella *et al.*<sup>32,33</sup>)

$$K_{ft} = \frac{\sigma_{max}}{\sigma_b} = \frac{\sigma_{cont}}{\sigma_b} + 1 = 1 + \frac{8}{\pi} \frac{\bar{p}}{\sigma_b} k \sqrt{f Q/P}, \quad (17)$$

where  $k$  is a contact geometrical factor equal to 1 in the Hertz contact case, and increasingly greater for rounded flat geometries towards the flat indenter case. Notice that, again, as a result of the independent bulk and contact loading factors, the latter equation is implicit on  $K_{ft}$ . But again, by reasoning in terms of the non-dimensional ratios  $R_p, R_q$  and  $f$  and rearranging, we get

$$K_{ft}(R_p, R_q, f, k) = 1 + \frac{8}{\pi} R_p k \sqrt{f R_q}, \quad (18)$$

and  $K_{ft}$  does depend on all three non-dimensional factors, plus a geometrical factor, but obviously does not depend on the size of the contact. Finally, for full sliding,  $R_q = f$ , and the stress concentration reaches the maximum value.

**Implementation of the CLNA model: discussion**

By equating  $K_{ft}$  with the  $K_{ff}$  predictions we get an estimate of the size separating the ‘crack-like’ from the ‘blunt notch’ behaviours. Accordingly, we define size  $a_D$  by equating (Eqs (16) and (18)).

Obviously, anything that makes the  $K_{ft}$  lower, and the fictitious geometrical factor  $Y$  higher, renders the transitional size  $a_D$  smaller. For example,  $R_p$  tends to have similar effects, as it increases both (although not in exact proportion), while  $k$  only increases the numerator (this is because a sharper geometry increases the  $K_t$  but does not make any difference to  $Y$ ).

Clearly, the new CLNA model suggests to use the minimum of the two  $K_{ft}$ ,  $K_{ff}$ , hence we define the resulting global knock down factor in FF, simply  $K_f$ , according to the Atzori–Lazzarin criterion (1), as

$$K_f = \left\langle K_{ff} \left( R_p, R_q; f, \frac{a}{a_0} \right); K_{ft}(R_p, R_q, f, k) \right\rangle, \quad (19)$$

where again  $\langle a; b \rangle$  indicates the minimum between  $a, b$ . Alternatively, it could be written as  $K_{ff}$  for  $a < a_D$ , and  $K_{ft}$  for  $a > a_D$ . In the latter form, it permits some conclusions on the general effect of FF. Perhaps the most problematic aspect of FF has been the too high number of parameters involved to manage to separate the effects. Given a certain range of conditions in terms of geometry and the five parameters (bulk stress, pressure, tangential load, friction coefficient and contact area size), the maximum number of parameters effectively affecting the infinite life behaviour of the FF contact is four, and it is when the peak stress condition is acting. Otherwise in the crack-like range, the number of independent parameters is three, given by  $R_p$ ,  $R_q$  or  $f$ ,  $a/a_0$ . There are interesting aspects of this when varying one or other of the parameters. For example, when  $R_q$  is increased, then  $K_{ft}$  certainly increases, whereas  $K_{ff}$  only increases if we have not reached the limiting value given by  $f$ , and therefore  $a_D$  will generally tend to increase. More details on  $a_D$  will be given when the full CLNA diagram will be displayed in the following paragraphs.

**Validation of the CLNA model: comparison with Hertzian experiments**

Hertzian experiments on Al-alloy originally contained and discussed in Nowell's thesis<sup>35</sup> and on a typical aeronautical Ti-6Al-4V alloy are reported in details in Araùjo,<sup>36</sup> and Araùjo and Nowell,<sup>17,18</sup> where either short-crack or averaging techniques were proposed. Previously, the Nowell Al-alloy data have been used in comparison with other attempts of predictive methods, and in particular Fellows *et al.*,<sup>21</sup> Szolwinski and Farris<sup>16</sup> and Nowell and Hills.<sup>6</sup> They are very convenient therefore to discuss the capabilities of the method, with respect to previous attempts. In particular, Hertzian geometry gives a condition sufficiently remote from the sharp flat geometry for most practical realistic conditions permitting a significant validation of the present method. Also, they are obtained in well-controlled conditions, with friction coefficient measured as an average value in the contact area and inferred

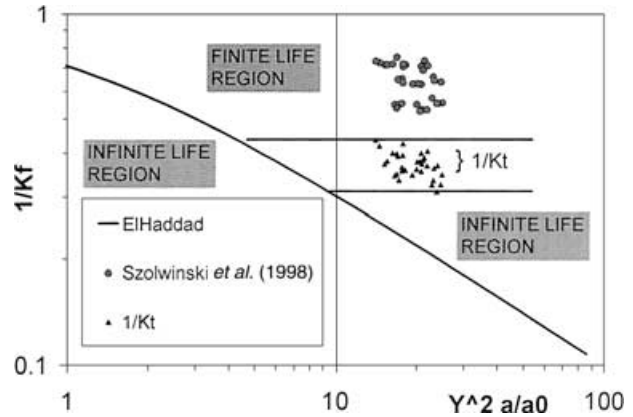


**Fig. 5** Prediction of the CLNA model for the Szolwinski *et al.*<sup>16</sup> experiments ( $\Delta\sigma_L = 308$  MPa, and  $\Delta K_{th} = 4.2$  MN m<sup>-3/2</sup>, giving  $a_0 = 59$   $\mu$ m). The data fall all in the finite life region, as confirmed by the CLNA prediction, which also shows they are remote from the stress concentration factor regime.

in the microslip area. In these experiments, infinite life is obtained by progressively reducing the size of the contact, following an idea originally proposed by Bramhall,<sup>37</sup> i.e., maintaining all other average stress field values constant. Most other data in the literature are either presented as SN data for relatively short lives, or other conditions are not reported. For example, Szolwinski *et al.*<sup>16</sup> report 37 experiments with a similar Al-alloy, Al2024-T351,<sup>†</sup> all failed well before 10<sup>6</sup> cycles, and the CLNA correctly predicts failure (finite life) for all of them (see Fig. 5).

It is worth spending a few more words on Fig. 5, as it is the first example of the  $K_f$  'diagram' using the CLNA model, and a few general remarks are not misplaced. Given we are about to compare with experimental data points, which are likely to have various  $Y$  factors, the factor  $Y^2 a/a_0$  is used on the abscissae, so that the El Haddad Eq. (16) for the crack-like behaviour is simply a single line clearly marking the region of infinite life irrespective of the peak stress condition. A second region of infinite life is obtained above the El Haddad line, for those conditions giving a peak stress lower than the fatigue limit—this second region is therefore enclosed between the El Haddad line and the particular horizontal line corresponding to the  $K_f = K_{ft}$  condition. In particular, in the case of Szolwinski *et al.*<sup>16</sup> data, each data has a slightly different peak stress, so that a number of data points are represented in the diagram for the  $K_f = K_{ft}$  condition. However, they all give a peak stress corresponding to a  $K_{ft}$  factor around 2.5–3, and two horizontal lines mark upper and lower limits. The experimental data anyway all fall well within the finite life region.

<sup>†</sup>A fatigue limit range of 308 MPa, and long crack threshold range of 4.2 MN m<sup>-3/2</sup> were considered, giving an  $a_0 = 59$   $\mu$ m.

**Table 1** Nowell's fretting fatigue tests with Al-4%Cu and Ti-6Al-4V (taken from Refs [17, 18, 36])

Mat and series exp	$f$	$p_0$ (MPa)	$Q/P$	$\sigma_b$ (MPa)	$\sigma_{cont}$ (MPa)	$\sigma_{max}$ (MPa)	$N_f (\times 10^6)$	$a$ (mm)	$R_p$	$Y$
Al 1	0.8 “	157 “	0.45 “	92.7 “	188	281	1.29	0.38	1.694	0.631
							0.67	0.57		
							0.85	0.76		
							0.73	0.95		
							0.67	1.14		
							>10	0.1		
							>10	0.19		
>10	0.28									
Al 3	0.8 “	143 “	0.45 “	92.7 “	172	264	>10	0.09	1.543	0.597
							>10	0.18		
							4.04	0.27		
							1.5	0.36		
							0.8	0.54		
							0.61	0.72		
							1.24	0.9		
							0.69	1.08		
Al 4	0.8 “	143 “	0.45 “	77.2 “	172	249	>10	0.09	1.852	0.667
							>10	0.18		
							1.2	0.36		
							1.42	0.54		
							0.61	0.72		
							1.24	0.9		
Al 5	0.75 “	120 “	0.45 “	61.8 “	139	201	>10	0.14	1.942	0.687
							>10	0.21		
							>10	0.28		
							>10	0.42		
							>10	0.57		
							1.57	0.71		
1.23	0.85									
Ti 6 - 4	0.5 “	650 “	0.16 “	280 “	368	648	>1.4	0.25	2.321	0.436
							0.521	0.76		
							0.374	1.01		
							0.196	1.22		
							0.173	1.42		

The CLNA model will then be applied to the data of Araujo and Nowell,<sup>4,17,18,‡</sup> briefly summarized in Table 1. We notice that in Nowell's experiment, for each series, the bulk stress as well as the pressure are kept constant, but the ratio between the two is not, i.e.,  $R_p$  is not constant (however, only moderately varying, as  $R_p = 1.69, 1.54, 1.85, 1.94$ , for Al series 1, 3, 4, 5, respectively, and  $R_p = 2.32$ , for the Ti single series). Regarding  $R_q$ , it is constant for the Al-series experiment ( $R_q = 0.45$ ) and, independently, for the Ti experiments ( $R_q = 0.16$ ). This is taken care of in the calculation of the factor  $Y$ , which permits the single

diagram of Fig. 6, by using the abscissa  $Y^2 a/a_0$ , to represent all the limiting behaviour as a single El Haddad line. The  $K_t$  lines, are various and depend on each combination of  $(R_p, R_q, f, k)$ . Notice that all points fall well above the  $K_t$  lines and failures and runout are correctly separated by the El Haddad line with the exception of a single point at the highest level of bulk stress, where the experimental results are also ambiguous. The agreement with the CLNA model therefore appears excellent. Notice that as material properties, we have only used two most widely available data, i.e., the fatigue limit in alternate tension and the fatigue threshold for long cracks in mode I. The excellent agreement with the experiments suggests therefore that, at least within these ranges of conditions, the

<sup>‡</sup>From which a fatigue limit range of 248 MPa, and long crack threshold range of  $4.2 \text{ MN m}^{-3/2}$  were considered, giving an  $a_0 = 91 \mu\text{m}$ .

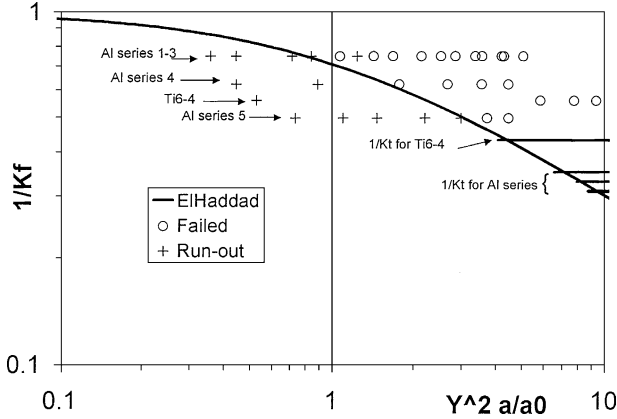


Fig. 6 Comparison of Nowell's experiments (Nowell 1988; Araújo and Nowell 1999, 2002, giving  $a_0 = 91 \mu\text{m}$ ,  $25 \mu\text{m}$  for Al and Ti alloys, respectively) with predictions of the CLNA model. Notice only 1 (dubious) experimental point fails the comparison out of 33. The  $1/K_t$  lines are obtained for the given ratios  $R_p$  of the various series of experiments. All the data fall in the crack-like region.

multiaxiality of fretting is only of negligible importance, and that the constant normal load does not significantly alter the threshold condition either. Multiaxial parameters, as used by Szolwinski *et al.*<sup>16</sup> and Araújo and Nowell,<sup>17,18</sup> do not seem necessary at this stage, within the limits of the experiments under consideration. Also, having written the initiation condition very simply in terms of contact sizes and loads permits interesting examination of various effects, as considered in the next section.

**THE CLNA-MODEL 'FF DIAGRAM'**

In contrast to the standard fatigue case where the nominal stress is clearly defined and there is no other loading condition, in our CLNA model for FF, we have been able to represent a single diagram by using the non-dimensional ratios ( $R_p, R_q, f, k$ ). The corresponding diagram shows how the FF performance is expected to decrease with increasing size of the contact, but maintaining the ratios ( $R_p, R_q, f$ ) constant. More often, one is interested to know what is the effect of changing only one or the other of the ratios. For example, what is expected to happen when only tangential load is increased, or friction, or pressure, or bulk stress. For example, if we keep the pressure constant, and assuming we are in the region of partial slip for the CA model, we would have from Eq. (13)

$$K_{ff}^2 = 1 + \left(\frac{2 f \bar{p}}{\pi \sigma_b}\right)^2 \frac{a}{a_0} = 1 + \left(\frac{2 f \bar{p}}{\pi \sigma_L} K_{ff}\right)^2 \frac{a}{a_0}, \quad (20)$$

where we have the notation in terms of amplitude for fatigue limit,  $\sigma_L$ , instead of the range. This is an implicit equation for the factor  $K_{ff}$ , and rearranging gives

$$K_{ff} = 1 / \sqrt{1 - \left(\frac{2 f \bar{p}}{\pi \sigma_L}\right)^2 \frac{a}{a_0}}. \quad (21)$$

Notice that  $K_{ff}$  depends now on three non-dimensional factors only: the ratio  $p/\sigma_L$ , where with respect to the previous pressure ratio, we have divided the pressure by the fatigue limit instead of the bulk stress; the friction coefficient  $f$ ; and the crack size ratio,  $a/a_0$ , and does not depend on  $Q/P$ . Also, notice that this solution is valid for

$$\frac{a}{a_0} < 1 / \left(\frac{2 f \bar{p}}{\pi \sigma_L}\right)^2. \quad (22)$$

This condition is simply the counterpart of reasoning for a fixed average pressure  $p$ . The total load, upon an increase of the contact area, becomes larger, and this renders the condition increasingly more severe. In fact, simply when condition (22) is met, the threshold fracture mechanics condition is met, with zero bulk stress, just because of  $\Delta K_{II} = (2/\pi)\Delta q \sqrt{\pi a} = \Delta K_{th}$ . Similarly, for the  $K_{ft}$  factor, we rewrite Eq. (17) as

$$K_{ft} = 1 + \frac{8 \bar{p}}{\pi \sigma_b} K_{ft} k \sqrt{f Q/P}, \quad (23)$$

and again, the equation is implicit on  $K_{ft}$ . By rearranging, we get

$$1/K_{ft} = 1 - \frac{8 \bar{p}}{\pi \sigma_L} k \sqrt{f Q/P}, \quad (24)$$

and as  $K_{ft} > 1$ , and  $1/K_{ft} > 0$ , follows that this solution is valid for

$$1 < \frac{8 \bar{p}}{\pi \sigma_L} k \sqrt{f Q/P}. \quad (25)$$

A limiting condition occurs this time because when condition (25) is met,  $K_{ft} \rightarrow \infty$ , just because of contact loads and there is no truncation to use to the previous 'crack-like' condition.

Other such curves may be obtained by fixing, say, total load  $P$ , i.e., imposing the average pressure to be inversely proportional to contact area size, and so on. However, rather than using a different plot for each condition, it may be easier to visualize the possible variations by using the original plot, with  $Y$  removed from the abscissae axis, and various curves for the various combinations of ratios ( $R_p, R_q, f, k$ ) plotted at once. Figure 7 shows a few examples of the resulting behaviour. The case of incipient full slip is chosen for simplicity, varying  $R_q = f = 0.1, 0.2, \dots, 1$  and having Hertzian geometry and Fig. 8 shows the same cases for a flatter geometry (namely  $k = 5$ , i.e., having five times higher contact stress concentration), and within each series of three, the pressure ratio is varied  $R_p = 1, 5, 10$ . Clearly the only difference between the two series of three plots is in the  $K_t$  lines, which truncate the El Haddad crack-like behaviour lines for larger contact sizes

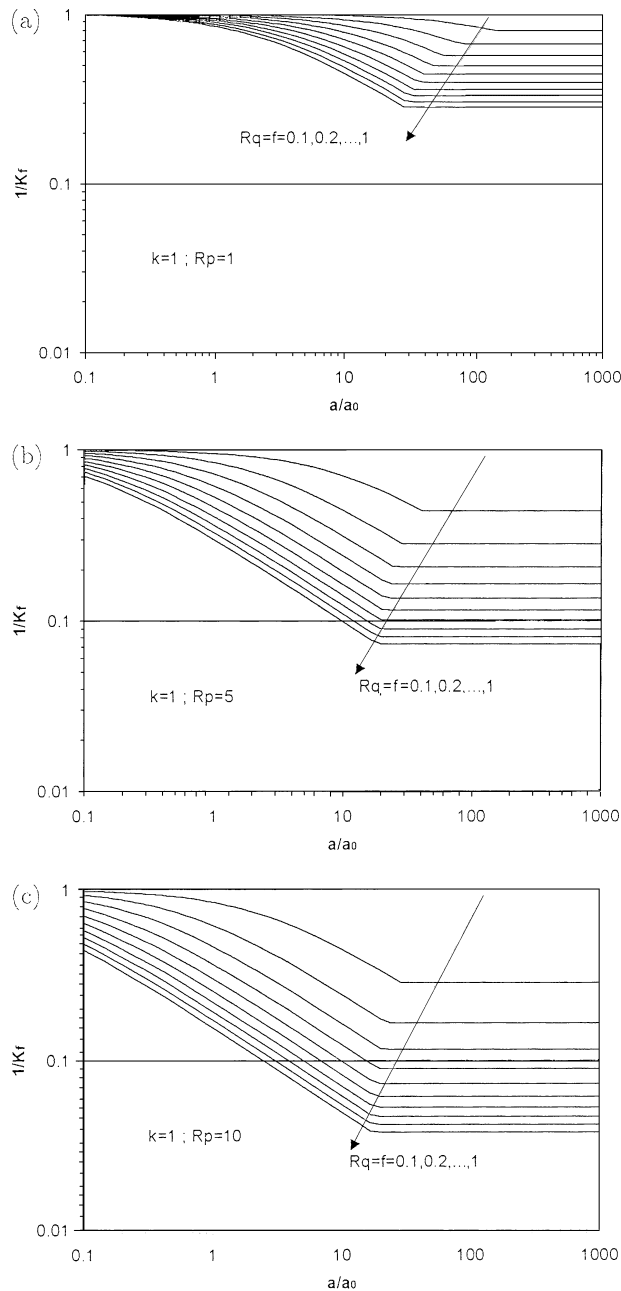


**Fig. 7** Theoretical predictions of the CLNA model for the case of incipient full slip  $R_q = f = 0.1, 0.2, \dots, 1$  for Hertzian geometry ( $k = 1$ ), with  $R_p = 1, 5, 10$  in cases (a), (b) and (c), respectively.

if the stress concentration is higher. In particular, it is noticed that the crack-like behaviour continues up to at least  $a/a_0 = 20$  for the cases represented in the Hertzian case, and up to an even much larger value ( $a/a_0 = 200$  or so) for the flatter geometry. This would make the blunt notch behaviour quite difficult to achieve in practise (meaning the pure stress concentration criterion would be extremely conservative in most cases), particularly for many practi-

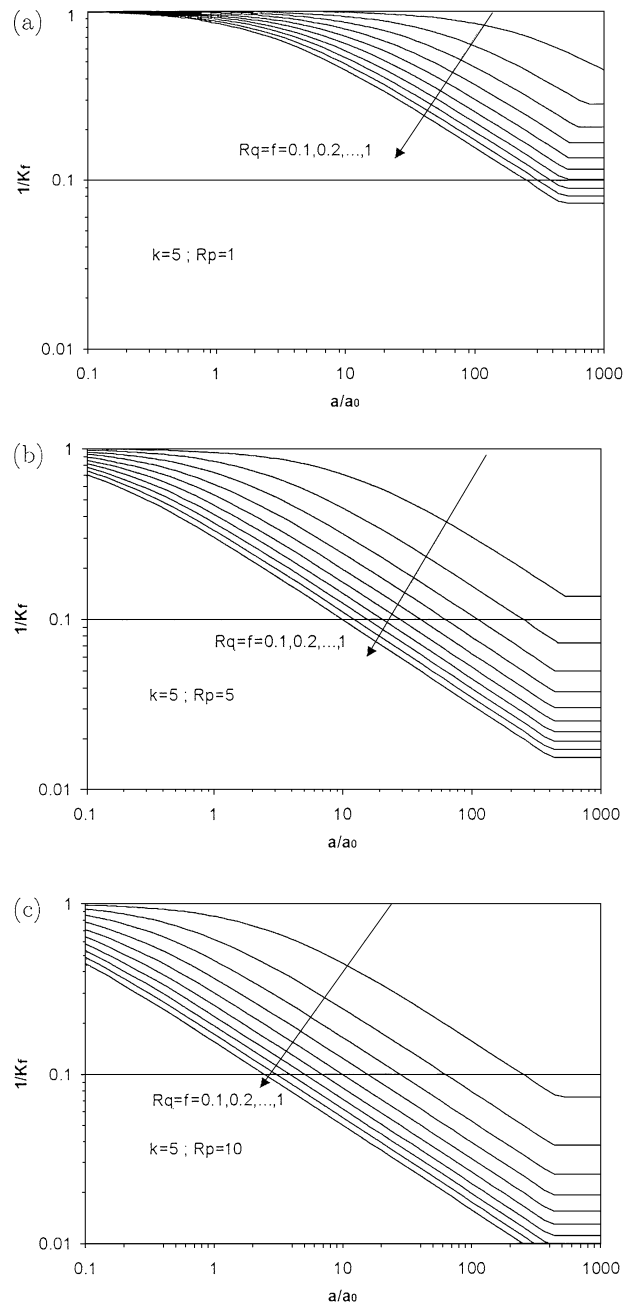


**Fig. 8** Same as Fig. 7 for a flatter geometry (namely  $k = 5$ , i.e., having five times higher contact stress concentration).

cal cases, like dovetail attachments in turbine blade joints, where the geometry is considerably flatter than Hertzian. For Al- or Ferrous alloys, having  $a_0$  of the order of  $100 \mu\text{m}$  or so, this would mean contact areas half-widths of the order 2 and 20 mm, respectively, whereas for Ti-alloys, sizes four times smaller.

Within each of the three pressure ratios, the variation is very significant, particularly moving from  $R_p = 1$  to  $R_p = 5$ .

## CONCLUSIONS

A new CLNA model has been derived for FF safe life design, using the Atzori–Lazzarin criterion<sup>26,28</sup> for fatigue in the presence of geometrical notches and cracks. Since the Atzori–Lazzarin criterion has proved very simple but also more accurate than a number of standard criteria such as Neuber, Peterson, Lukas–Klesnil as confirmed by direct comparisons with a wide range of data from the literature (see Atzori *et al.*<sup>28</sup> and Ciavarella and Meneghetti<sup>38</sup>), its application to fretting becomes particularly helpful, as it improves and combines features of previous crack and notch analogue models developed at MIT.

In particular, for small to intermediate contact area sizes, a corrected and generalized version of the CA model is proposed; the infinite-life threshold for FF *does not* depend on geometrical features of the contact, but depends only on three non-dimensional quantities: first, on the ratio  $a/a_0$  size of the contact to intrinsic material constant; then, on  $R_p$  (the ratio average pressure to bulk stress), and either  $R_q$  (the ratio tangential to normal load) or  $f$ , the friction coefficient. Only for large enough contact areas ( $a > a_D$ ), is the fretting life expected to depend on stress concentration (basically like in a NA model based on pure stress concentration) and in particular on all three ratios ( $R_p R_q$  and  $f$ ), as well as the details of the geometry of the contact.

The CLNA model is validated with classical Hertzian experiments, showing it may be considered simpler but not less accurate than previous attempts to predict initiation life, including recent averaging techniques. With respect to the latter, the empirical fitting constants are removed. Fretting fatigue seems to be, within the range of experiments considered, simply fatigue from a stress raiser feature, as such simply predicted by the fatigue limit (in tension) and mode I fatigue threshold for long cracks, which are generally available material properties.

## REFERENCES

- Tomlinson, G. A. (1927) The rusting of steel surfaces in contact. *Proc. R. Soc. London A*, **115**, 472–483.
- Eden, E. M., Rose, W. N. and Cunningham, F. L. (1911) The endurance of metals. *Proc. Inst. Mech. Engrs* **875**, 68–76.
- Gillet, H. M. and Mack, E. L. (1924) Notes on some endurance tests of metals. *Proc. Am. Soc. Test. Mat.* **24**, 476.
- Nishioka, K., Nishimura, S. and Hirakawa, K. (1968) Fundamental investigation of fretting fatigue: Part 1. On the relative slip amplitude of press-fitted axle assemblies. *Bull. JSME* **11**, 437–445.
- Nishioka, K. and Hirakawa, K. (1969) Fundamental investigation of fretting fatigue: Part 3. Some phenomena and mechanism of surface cracks: Part 4. The effect of mean stress: Part 5. The effect of relative slip amplitude. *Bull. JSME* **12**, 397–407, 408–414, 692–697.
- Nowell, D. and Hills, D. A. (1990) Crack initiation criteria in fretting fatigue. *Wear* **136**, 329–343.
- Ruiz, C., Buddington, P. H. B. and Chen, K. C. (1984) An investigation of fatigue and fretting in a dovetail joint. *Exp. Mech.* **24**, 208–217.
- Ruiz, C. and Chen, K. C. (1986) Life assessment of dovetail joints between blades and discs in aero-engines. In: *Proceedings of International Conference on Fatigue*. Sheffield, ImechE, London.
- Warlow-Davis, E. J. (1941) Fretting corrosion and fatigue strength: Brief results of preliminary experiments. *Proc. Inst. Mech. Engrs* **146**, 32–40.
- McDowell, J. R. (1953) Fretting Corrosion. ASTM STP 144, Philadelphia, PA pp. 24–39.
- Lindley, T. C. (1997) Fretting fatigue in engineering alloys. *Int. J. Fat.* **19** (Suppl. 1), S39–S49.
- Johnson, K. L. and O'Connor, J. J. (1964) *Mechanics of Fretting*. Applied Mechanics Convention Newcastle 14–17 April 1964. Paper 11 published by Institute of Mechanical Engineering, London.
- Wright, G. P. and O'Connor, J. J. (1972) The influence of fretting and geometric stress concentrations on the fatigue strength of clamped joints. *Proc. Inst. Mech. Eng.* **186**, 827–833.
- Giannakopoulos, A. E., Lindley, T. C. and Suresh, S. (2000) Similarities of stress concentration in contact at round punches and fatigue at notches: Implication to fretting fatigue crack initiation. *Fat. Fract. Engng Mat. Struct.* **23**, 561–571.
- Neu, R. W., Pape, J. A. and Swalla, D. R. (1999) Methodologies for linking nucleation and propagation approaches for predicting life under fretting fatigue. *Fretting Fatigue: Current Technologies and Practices*. ASTM STP 1367 (Edited by D. W. Hoepfner, V. Chandrasekaran and C. B. Elliot). American Society for Testing and Materials, West Conshohocken, PA.
- Szolwinski, M. P. and Farris, T. N. (1998) Observation, analysis and prediction of fretting fatigue in 2024-T351 aluminum alloy. *Wear* **221**, 24–36.
- Araújo, J. A. and Nowell, D. (1999) Analysis of pad size effects in fretting fatigue using short crack arrest methodologies. *Int. J. Fatigue* **21**, 947–956.
- Araújo, J. A. and Nowell, D. (2002) The effect of rapidly varying contact stress fields on fretting fatigue. *Int. J. Fatigue* **24**, 763–775.
- Endo, K. and Goto, H. (1976) Initiation and propagation of fretting fatigue cracks. *Wear* **38**, 311–324.
- Waterhouse, R. B. (1981) *Fretting Fatigue*. Applied Science Publishers Ltd., London.
- Fellows, L. J., Nowell, D. and Hills, D. A. (1997) Analysis of crack initiation and propagation in fretting fatigue: The effective initial flaw size methodology. *Fat. Fract. Eng. Mat. Struct.* **20**, 61–70.
- Giannakopoulos, A. E., Lindley, T. C. and Suresh, S. (1998) Overview N.129, Aspects of equivalence between contact mechanics and fracture mechanics: Theoretical connections and a life-prediction methodology for fretting-fatigue. *Acta Mater.* **46**, 2955–2968.
- Mugadu, A., Hills, D. A. and Limmer, L. (2002) An asymptotic approach to crack initiation in fretting fatigue of complete contacts. *J. Mech. Phys. Solids* **50**, 531–547.
- Giannakopoulos, A. E., Venkatesh, T. A., Lindley, T. C. and Suresh, S. (1999) The role of adhesion in contact fatigue. *Acta Mater.* **47**, 4653–4664.

- 25 Smith, R. A. and Miller, K. J. (1978) Prediction of fatigue regimes in notched components. *Int. J. Mech. Sci.* **20**, 201–206.
- 26 Atzori, B. and Lazzarin, P. (2001) Notch sensitivity and defect sensitivity under fatigue loading: Two sides of the same medal. *Int. J. Fract.* **107**, L3–L8.
- 27 El Haddad, M. H., Topper, T. H. and Smith, K. N. (1979) Prediction of Non-Propagating Cracks. *Eng. Fract. Mech.* **11**, 573–584.
- 28 Atzori, B., Lazzarin, P. and Meneghetti, G. (2003) Fracture Mechanics and notch sensitivity. *Fat. Fract. Eng. Mat. Struct.* **26**, 257–267.
- 29 Ciavarella, M. and Macina, G. (2003) A note on the Crack Analogue model for fretting fatigue, *Int. J. Solids Struct.* **40**, 807–825.
- 30 Ciavarella, M., Demelio, G. and Hills, D. A. (1999) *The Use of Almost Complete Contacts for Fretting Fatigue Tests, Fatigue and Fracture Mechanics*. ASTM STP 1332 (Edited by T. L. Panontin and S. D. Sheppard). Vol. 29, American Society for Testing and Materials, West Conshohocken, PA, pp. 696–709.
- 31 Ciavarella, M. and Demelio, G. (2001) A review of analytical aspects of fretting fatigue, with extension to damage parameters, and application to dovetail joints. *Int. J. Solids Struct.* **38**, 1791–1811.
- 32 Ciavarella, M. and Macina, G. (2003) New results for the fretting-induced stress concentration on Hertzian and flat rounded contacts. *Int. J. Mech. Sci.* **45**, 449–467.
- 33 Ciavarella, M., Macina, G. and Demelio, G. (2002) On stress concentration on nearly flat contacts. *J. Strain Anal. Eng.* **37**, 493–501.
- 34 Ciavarella, M., Hills, D. A. and Monno, G. (1998) The influence of rounded edges on indentation by a flat punch. *IMechE part C - J. Mech. Eng. Sci.* **212**, 319–328.
- 35 Nowell, D. (1988) *An Analysis Of Fretting Fatigue*. DPhil Thesis, University of Oxford, Oxford.
- 36 Araujo, J. A. (2000). *Prediction of Fretting Fatigue Crack Initiation Using Multiaxial Fatigue Criteria*. DPhil Thesis, Oxford University.
- 37 Bramhall, R. (1973) *Studies in Fretting Fatigue*. DPhil Thesis, University of Oxford.
- 38 Ciavarella, M. and Meneghetti, G. (2003) On fatigue limit in the presence of notches: Classical versus recent formulations. *Int. J. Fat.* (in press).